

# Linköping University Post Print

## Relating the open-circuit voltage to interface molecular properties of donor:acceptor bulk heterojunction solar cells

Koen Vandewal, Kristofer Tvingstedt, Abay Gadisa, Olle Inganäs and Jean V Manca

N.B.: When citing this work, cite the original article.

Original Publication:

Koen Vandewal, Kristofer Tvingstedt, Abay Gadisa, Olle Inganäs and Jean V Manca, Relating the open-circuit voltage to interface molecular properties of donor:acceptor bulk heterojunction solar cells, 2010, PHYSICAL REVIEW B, (81), 12, 125204.

<http://dx.doi.org/10.1103/PhysRevB.81.125204>

Copyright: American Physical Society

<http://www.aps.org/>

Postprint available at: Linköping University Electronic Press

<http://urn.kb.se/resolve?urn=urn:nbn:se:liu:diva-54852>

## Relating the open-circuit voltage to interface molecular properties of donor:acceptor bulk heterojunction solar cells

Koen Vandewal,<sup>1,\*</sup> Kristofer Tvingstedt,<sup>2</sup> Abay Gadisa,<sup>1</sup> Olle Inganäs,<sup>2</sup> and Jean V. Manca<sup>1</sup>

<sup>1</sup>IMEC-IMOMEC, vzw and Institute for Materials Research, Hasselt University, Wetenschapspark 1, 3590 Diepenbeek, Belgium

<sup>2</sup>Biomolecular and Organic Electronics, Center of Organic Electronics (COE), Department of Physics, Chemistry and Biology, Linköping University, 58183 Linköping, Sweden

(Received 18 September 2009; revised manuscript received 3 February 2010; published 10 March 2010)

The open-circuit voltage ( $V_{oc}$ ) of polymer:fullerene bulk heterojunction solar cells is determined by the interfacial charge-transfer (CT) states between polymer and fullerene. Fourier-transform photocurrent spectroscopy and electroluminescence spectra of several polymer:fullerene blends are used to extract the relevant interfacial molecular parameters. An analytical expression linking these properties to  $V_{oc}$  is deduced and shown to be valid for photovoltaic devices comprising three commonly used conjugated polymers blended with the fullerene derivative [6,6]-phenyl-C61-butyric acid methyl ester (PCBM).  $V_{oc}$  is proportional to the energy of the CT states  $E_{CT}$ . The energetic loss  $q\Delta V$  between  $E_{CT}$  and  $qV_{oc}$  vanishes when approaching 0 K. It depends linearly on  $T$  and logarithmically on illumination intensity. Furthermore  $q\Delta V$  can be reduced by decreasing the electronic coupling between polymer and fullerene or by reducing the nonradiative recombination rate. For the investigated devices we find a loss  $q\Delta V$  of  $\sim 0.6$  eV at room temperature and under solar illumination conditions, of which  $\sim 0.25$  eV is due to radiative recombination via the CT state and  $\sim 0.35$  eV is due to nonradiative recombination.

DOI: [10.1103/PhysRevB.81.125204](https://doi.org/10.1103/PhysRevB.81.125204)

PACS number(s): 71.35.Gg, 72.40.+w, 72.80.Rj, 73.50.Pz

### I. INTRODUCTION

Research in organic photovoltaics has advanced over the recent years. Currently power conversion efficiencies of 5% to above 7%, with external quantum efficiencies of 70–80% (Refs. 1–5) and internal quantum efficiencies approaching 100%, are achieved for polymer:fullerene photovoltaic devices. This indicates that in these high quantum efficiency cases, nearly all photons absorbed by the polymer are converted into collected electrons at short circuit and, hence, that the achieved short-circuit currents are close to their predicted maximum. Power conversion efficiency, however, does not only depend on the production of photocurrent but also on the photovoltage. Optimization and understanding of the fundamental limits of the open-circuit voltage ( $V_{oc}$ ) therefore are as important as the optimization of the short-circuit current ( $J_{sc}$ ).

$V_{oc}$  has been shown to depend on the donor/acceptor material combination,<sup>6,7</sup> the electrode material,<sup>8</sup> as well as light intensity and temperature.<sup>9</sup> Modeling of the internal field and charge distribution has successfully explained the influence of several of these parameters on  $V_{oc}$ . However, there exists also a relation between externally measurable electro-optical spectra and  $V_{oc}$ .<sup>10</sup> This relation is based on the principle of detailed balance and the assumption of quasiequilibrium conditions.<sup>11,12</sup> A benefit of this approach is that it avoids description of the internal charge and field distributions in the solar cell, which are difficult to measure. With this theory, the origin of  $V_{oc}$  of polymer:fullerene solar cells can be explained in terms of ground-state charge-transfer complex (CTC) formation between polymer and fullerene.<sup>10</sup>

Upon blending a suitable donor polymer with a fullerene acceptor, interaction between polymer and fullerene results in the formation of a ground-state CTC.<sup>13–22</sup> Upon excitation of this new ground state, the CT exciton is created. Optical

transitions from the CTC ground state to the CT exciton are visible in the low-energy region of the photovoltaic external quantum efficiency ( $EQE_{PV}$ ) spectrum if measured with sensitive techniques.<sup>18</sup> Radiative decay of CT excitons is sometimes observed in photoluminescence measurements of polymer:fullerene blends<sup>14–16,19–22</sup> and can be more easily detected in electroluminescence (EL) spectra obtained by applying a forward voltage over polymer:fullerene photovoltaic devices.<sup>21</sup>

CT excitons play a major role in the operation of polymer:fullerene solar cells.<sup>10,14,19,22</sup> These weakly bound electron-hole pairs at the polymer:fullerene interface are mainly populated via a photoinduced electron transfer after excitation of polymer or fullerene. Due to the low oscillator strength of polymer:fullerene CTCs only a very small fraction of CT excitons is populated by direct optical excitation of the CTCs. The major contribution to the photocurrent originates from polymer or fullerene excitation. However, the efficiency of CT exciton formation and their dissociation into free carriers determines the photocurrent.<sup>14,19,22</sup> Both formation and dissociation efficiencies depend on the blend morphology and donor:acceptor energetics. Also  $V_{oc}$  is determined by the spectral properties of the CT excitons, again being morphology dependent. In general, the spectral position of the CT exciton correlates with the difference between the lowest unoccupied molecular orbital (LUMO) of the fullerene acceptor and the highest occupied molecular orbital (HOMO) of the donor polymer,<sup>23</sup> resulting in the widely observed correlation between  $V_{oc}$  and this difference.<sup>1,2,6,7</sup> However, recently it has been argued that other CTC related parameters, such as the electronic coupling between donor and acceptor, also have an influence on  $V_{oc}$ .<sup>24,25</sup>

In this paper we aim to describe in more detail how  $V_{oc}$  is affected by CTC properties. These properties are obtained by observing the CT optical transition bands in sensitive mea-

measurements of the photovoltaic external quantum efficiency ( $EQE_{PV}$ ) spectrum and the EL spectrum. An analytical expression for  $V_{oc}$  as a function of interfacial CTC properties is deduced.  $V_{oc}$  is shown to be proportional to the energy of the interfacial CT state  $E_{CT}$ . The energetic loss between  $E_{CT}$  and  $qV_{oc}$  depends linearly on temperature and logarithmically on illumination intensity as observed also by others.<sup>9,26</sup> In this work we show that this loss can be reduced by reducing the electronic coupling between polymer and fullerene and by reducing the nonradiative recombination.

The derived analytical expression is shown to be valid in a temperature range from 150 to 300 K and under different illumination intensities, for four material systems, consisting of poly[2-methoxy-5-(30,70-dimethyloctyloxy)-1,4-phenylene vinylene] (MDMO-PPV), poly[3-hexylthiophene] (P3HT), and poly[2,7-(9-di-octyl-fluorene)-alt-5,5-(4',7'-di-2-thienyl-2',1',3'-benzothiadiazole)] (APFO3), blended with the fullerene derivative [6,6]-Phenyl C61 butyric acid Methyl ester (PCBM). For the APFO3 based devices, APFO3:PCBM 1:4 and 1:1 stoichiometries were studied.

## II. THEORY

In the framework of Marcus theory, the spectral lineshape of the CT absorption cross section  $\sigma(E)$  at photon energy  $E$  is described by<sup>27,28</sup>

$$\sigma(E)E = \frac{f_{\sigma}}{\sqrt{4\pi\lambda kT}} \exp\left(\frac{-(E_{CT} + \lambda - E)^2}{4\lambda kT}\right) \quad (1)$$

Hereby is  $k$  Boltzmann's constant and  $T$  is the absolute temperature.  $E_{CT}$  is the free-energy difference between the CTC ground state and the CT excited state and  $\lambda$  is a reorganization energy associated with the CT absorption process, as shown in Fig. 1(a).  $f_{\sigma}$  does not depend on  $E$  (Ref. 28) and is proportional to the square of the electronic coupling matrix element. It represents a measure of the strength of the donor/acceptor material interaction. The absorption coefficient  $\alpha$  in the spectral region of CT absorption equals  $\sigma N_{CTC}$ , with  $N_{CTC}$  as the number of CTCs per unit volume.

The emission rate  $I_f$  at photon energy  $E$ , per unit energy equals<sup>27,28</sup>

$$\frac{I_f}{E} = \frac{f_{I_f}}{\sqrt{4\pi\lambda kT}} \exp\left(\frac{-(E_{CT} - \lambda - E)^2}{4\lambda kT}\right). \quad (2)$$

In analogy to  $f_{\sigma}$ ,  $f_{I_f}$  is not dependent on  $E$  and is proportional to the square of the electronic coupling matrix element.<sup>28</sup> The left-hand side of Eqs. (1) and (2) are called the reduced absorption and emission spectrum, respectively. They exhibit a mirror image relationship. The midpoint energy of these two spectra equals  $E_{CT}$ . In principle,  $\lambda$  can be deduced from the Stokes shift, or from the linewidth of the absorption or emission bands, by fitting with formulas (1) or (2). This is visualized in the scheme shown in Fig. 1(a). It should be noted however that in real materials, the Stokes shift can differ from  $2\lambda$  as a result of a disordered density of states, with emission taking place only from the lower-energy excited states.<sup>29</sup>

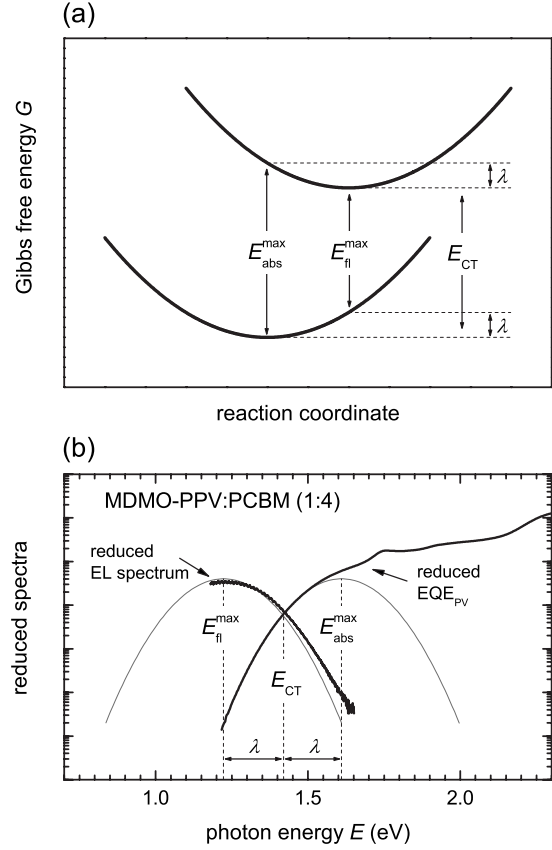


FIG. 1. (a) Free-energy diagram for the ground state and lowest excited state of the CTC as a function of a generalized coordinate. (b) Reduced  $EQE_{PV}$  and EL spectrum for a MDMO-PPV:PCBM (1:4) photovoltaic device. The gray curves are fits of the  $EQE_{PV}$  and EL spectra using formulas (1) and (2), using the same  $E_{CT}$  and  $\lambda$  values. These parameters, together with the maxima of absorption  $E_{abs}^{max}$  and emission  $E_{fl}^{max}$ , are indicated in the figure.

Because of their low absorption coefficients, highly sensitive techniques are needed to spectrally resolve CT absorption bands in polymer:fullerene blends.<sup>30</sup> We use Fourier-transform photocurrent spectroscopy (FTPS) to measure the photovoltaic  $EQE_{PV}$  spectrum of polymer:fullerene devices over several decades. The CT bands are visible in the low-energy part of the  $EQE_{PV}$  spectrum. Because of the low value of  $\alpha$ , the total absorption in this spectral region can be approximated by  $\alpha 2d$ , when using a back reflecting metal cathode. The  $EQE_{PV}$  equals the total absorption  $\alpha 2d$ , multiplied by the absorbed-photon-to-electron internal-conversion efficiency  $\eta$ ,

$$EQE_{PV}(E) = \eta \sigma(E) N_{CTC} 2d. \quad (3)$$

Using Eq. (1) for  $\sigma(E)$  we obtain in the spectral region of CT absorption,

$$EQE_{PV}(E) = \frac{f}{E \sqrt{4\pi\lambda kT}} \exp\left(\frac{-(E_{CT} + \lambda - E)^2}{4\lambda kT}\right) \quad (4)$$

In this equation the prefactor  $f$  equals  $\eta N_{CTC} 2d f_{\sigma}$ . The normalized reduced  $EQE_{PV}$  and EL emission spectra are shown in Fig. 1(b) for MDMO-PPV:PCBM in a 1:4 ratio. In

the figure we have indicated how the parameters  $E_{CT}$  and  $\lambda$  in Fig. 1(a) can be deduced from Fig. 1(b).

We will now relate these CTC properties to  $V_{oc}$ . In Ref. 10, using the method of detailed balance we have shown that the CT states relate to the dark current and  $V_{oc}$ . The following expression for the dark injected current  $J_{inj}$  versus voltage characteristic was used, with  $q$  being the elementary charge:

$$J_{inj} = J_0 \left[ \exp\left(\frac{qV}{kT}\right) - 1 \right]. \quad (5)$$

Hereby is implicitly assumed that  $J_0$  can still depend on the applied voltage or charge density present in the device. For the P3HT:PCBM material system, Shuttle *et al.* showed that, for voltages smaller or comparable to  $V_{oc}$ , this dark injected current  $J_{inj}$  constitutes recombination current only.<sup>31</sup> At  $V_{oc}$ , this recombination current balances with the photo-generated current  $J_{ph}$ , and  $V_{oc}$  is given by

$$V_{oc} = \frac{kT}{q} \ln\left(\frac{J_{ph}}{J_0} + 1\right) \quad (6)$$

Following the reasoning of Rau,<sup>12</sup>  $J_0$  is related to the electro-optical properties by

$$J_0 = \frac{q}{EQE_{EL}} \int EQE_{PV}(E) \phi_{BB}^T dE \quad (7)$$

Hereby is  $EQE_{EL}$  the EL external quantum efficiency and  $\phi_{BB}^T$  is the black body spectrum at temperature  $T$ . If in this expression [Eq. (7)],  $EQE_{PV}$  is evaluated at short circuit,  $J_{ph}$  in expression (6) should also be evaluated at short circuit using  $J_{ph} = J_{sc}$  in the evaluation of that equation.<sup>10</sup>

Further is the integral of the product  $\phi_{BB}^T EQE_{PV}$  of importance. Because  $\phi_{BB}^T$  is strongly decreasing with increasing energy, only the low-energy CT part of the  $EQE_{PV}$  spectrum contributes to this integral.<sup>10</sup> Using formula (4) in formula (7) gives

$$J_0 \approx \frac{q}{EQE_{EL}} f \frac{2\pi}{h^3 c^2} (E_{CT} - \lambda) \exp\left(-\frac{E_{CT}}{kT}\right). \quad (8)$$

The derivation of Eq. (8) is explained in more detail in the Appendix. From Eqs. (6) and (8) and with  $J_{ph} = J_{sc}$ , we get an analytical expression for  $V_{oc}$  as a function of  $EQE_{EL}$  and the parameters  $E_{CT}$ ,  $\lambda$  and  $f$ , evaluated at short circuit,

$$V_{oc} = \frac{E_{CT}}{q} + \frac{kT}{q} \ln\left(\frac{J_{sc} h^3 c^2}{f q 2\pi (E_{CT} - \lambda)}\right) + \frac{kT}{q} \ln(EQE_{EL}). \quad (9)$$

This formula implies a linear dependence of  $V_{oc}$  on temperature and a logarithmic dependence on illumination intensity. Such dependencies are observed and described in the literature.<sup>9,32,33</sup> The formulation of Eq. (9) however allows us to relate measurable properties related to the molecular interface between donor and acceptor to  $V_{oc}$ . This will be further discussed in the next sections.

### III. EXTRACTION OF CTC PROPERTIES

We have investigated polymer:PCBM solar cells based on three different donor polymers, i.e., MDMO-PPV, P3HT,

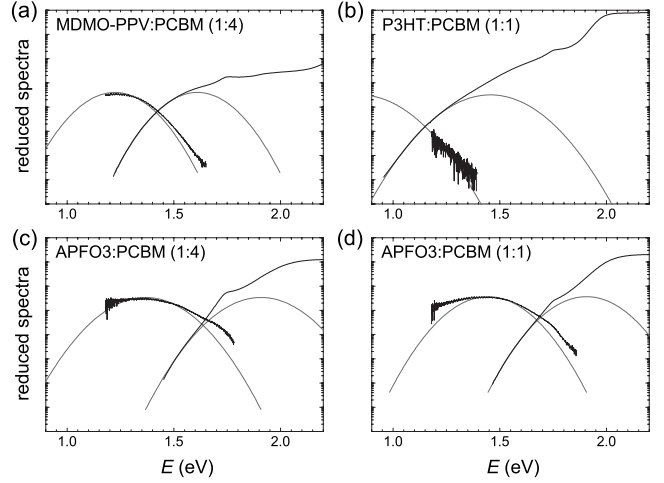


FIG. 2. Reduced  $EQE_{PV}$  and EL spectrum for (a) APFO3:PCBM (1:4), (b) APFO3:PCBM (1:1), and P3HT:PCBM (1:1) photovoltaic devices measured at room temperature. The gray curves are fits of the  $EQE_{PV}$  and EL spectra using formulas (1) and (2), with the same values for  $E_{CT}$  and  $\lambda$ .

APFO3. For the APFO3:PCBM blends, the polymer:fullerene 1:1 and 1:4 weight ratios are investigated. The  $EQE_{PV}$  and EL spectrum of MDMO-PPV:PCBM in a 1:4 ratio were already shown in Fig. 1(b). The spectra for the APFO3 and P3HT based devices are shown in Fig. 2.

For all material systems, we can deduce the reorganization energy  $\lambda$  and  $E_{CT}$  by fitting the CT band in the  $EQE_{PV}$  spectrum with Eq. (4). The EL emission spectra were measured with the aid of a Si charge couple device camera in the spectral range above 1.2 eV. In this range, the shape of the predicted reduced emission spectrum calculated via formula (2) resembles the measured reduced EL spectrum for all devices. The observed deviations from the predicted emission spectrum and the measured one are probably due to an increased effective temperature upon injecting current. Also effects related to a disordered density of states may contribute. However, we can conclude that the spectral shape of the CT bands at room temperature can be described to a fairly good approximation with formulas (1)–(4).

We have also applied formula (4) to account for the temperature dependence of the CT band.  $EQE_{PV}$  spectra were obtained between 150 and 300 K. The spectra for the four different material systems are shown in Fig. 3, together with their fits using formula (4). The obtained parameters are listed in Table I. The APFO3:PCBM blends show the highest  $E_{CT}$ , with the 1:1 stoichiometry having a slightly higher value than the 1:4 stoichiometry. The P3HT:PCBM blend has the lowest  $E_{CT}$  (Table I). For all studied material systems, we obtain  $\lambda$  values, which are quite independent of temperature, in the order of 0.2–0.3 eV. The values of  $E_{CT}$ , and the values of  $E_{abs}^{max}$  however, are slightly temperature dependent. We observe a small redshift of the CT band  $\sim 0.1$  eV upon cooling from 300 to 150 K. The exact origin of this phenomenon is not understood yet but corresponds to what is observed for the temperature dependence of the optical gap of pure conjugated polymers<sup>34,35</sup> or conjugated polymers involved in a

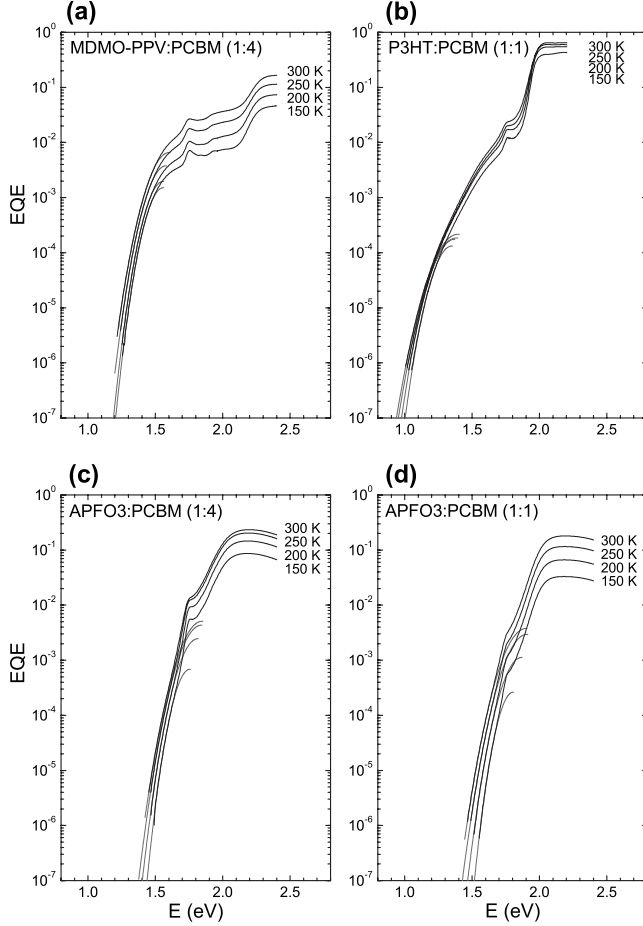


FIG. 3.  $EQE_{PV}$  spectra of (a) MDMO-PPV:PCBM (1:4), (b) P3HT:PCBM (1:1), (c) APFO3:PCBM (1:4), and (d) APFO3:PCBM (1:1) measured at several temperatures. The spectra were fitted with formula (4) to obtain values for  $E_{CT}$  and  $\lambda$ .

CTC.<sup>36</sup> The increase in the optical gap energy of pure materials upon increasing temperature was explained by the presence of an increased disorder at higher temperatures.<sup>36</sup>

#### IV. TEMPERATURE DEPENDENCE OF $V_{oc}$

In this section we investigate the temperature dependence of the dark saturation current  $J_0$  and  $V_{oc}$ . We have already seen that  $E_{CT}$  also depends on temperature. If we approximate  $E_{CT}$  by  $E_{CT}^0 + T \frac{dE_{CT}}{dT}$ , then, for the investigated devices  $\frac{dE_{CT}}{dT}$  is almost constant in the region from  $\sim 200$  to 300 K (Fig. 4). In this case  $E_{CT}^0$  is the intercept of the linear extrapolation of  $E_{CT}$  in the 200–300 K region, with the 0 K axis.  $E_{CT}^0$  is also the activation energy of the dark current, for  $J_0 \sim \exp(-\frac{E_{CT}^0 + T \frac{dE_{CT}}{dT}}{kT}) \sim \exp(-\frac{E_{CT}^0}{kT})$ .

We obtain the following values for  $E_{CT}^0$ : For MDMO-PPV:PCBM (1:4)  $E_{CT}^0 = 1.25$  eV and for P3HT:PCBM (1:1)  $E_{CT}^0 = 0.94$  eV. These values are very close to the activation energies  $E_a$  of the dark saturation current values found in Ref. 32 for MDMO-PPV:PCBM (1:4) ( $E_a = 1.25$  eV) and P3HT:PCBM (1:1) ( $E_a = 0.92$  eV–0.93 eV). For the APFO3:PCBM (1:4) and APFO3:PCBM (1:1) devices we find, respectively,  $E_{CT}^0 = 1.45$  eV and  $E_{CT}^0 = 1.51$  eV. This last example indicates that the spectral position of the CT band and  $E_{CT}$  are not only affected by the energetic levels of a single donor and a single acceptor molecule but also on polymer:fullerene stoichiometry.<sup>18</sup>

Regarding the temperature dependence of  $V_{oc}$ , Green (Ref. 37) showed that if the dark recombination current is of the form of Eq. (9), an approximately linear temperature dependence of  $qV_{oc}$  is predicted with a 0 K intercept equal to  $E_{CT}^0$ . In Fig. 4, the validity of this reasoning for the four polymer:fullerene solar cells investigated in this work is shown. This figure shows the temperature dependence of the  $E_{CT}$  values and  $V_{oc}$  values for different illumination intensities, between  $\sim 0.001$  and  $\sim 0.1$  sun. Extrapolation of temperature-dependent values  $E_{CT}$  to 0 K coincides very well with the extrapolation of the temperature-dependent  $V_{oc}$  for all four material systems and the investigated illumination intensities. For both APFO3 samples, there are some deviations from the straight line at low temperature. For inorganic solar cells, such as Si and GaAs, the same reasoning can be

TABLE I. Summary of the parameters  $E_{CT}$ ,  $\lambda$ , and  $f$  obtained by fitting the CT band in the temperature-dependent  $EQE_{PV}$  spectra with Eq. (4).

$T$ (K)	MDMO-PPV:PCBM(1:4)			P3HT:PCBM(1:1)		
	$f$ (eV <sup>2</sup> )	$E_{CT}$ (eV)	$\lambda$ (eV)	$f$ (eV <sup>2</sup> )	$E_{CT}$ (eV)	$\lambda$ (eV)
150	4.8E-4	1.31	0.25	4.1E-5	1.03	0.32
200	6.4E-4	1.36	0.20	6.0E-5	1.08	0.29
250	1.4E-3	1.39	0.19	7.2E-5	1.11	0.29
300	2.6E-3	1.42	0.19	8.8E-5	1.14	0.27
$T$ (K)	APFO3:PCBM(1:4)			APFO3:PCBM(1:1)		
	$f$ (eV <sup>2</sup> )	$E_{CT}$ (eV)	$\lambda$ (eV)	$f$ (eV <sup>2</sup> )	$E_{CT}$ (eV)	$\lambda$ (eV)
150	2.3E-4	1.54	0.22	9.0E-5	1.60	0.20
200	1.0E-3	1.58	0.24	4.9E-4	1.62	0.25
250	2.0E-3	1.61	0.24	1.5E-3	1.65	0.26
300	2.5E-3	1.64	0.21	2.0E-3	1.68	0.23

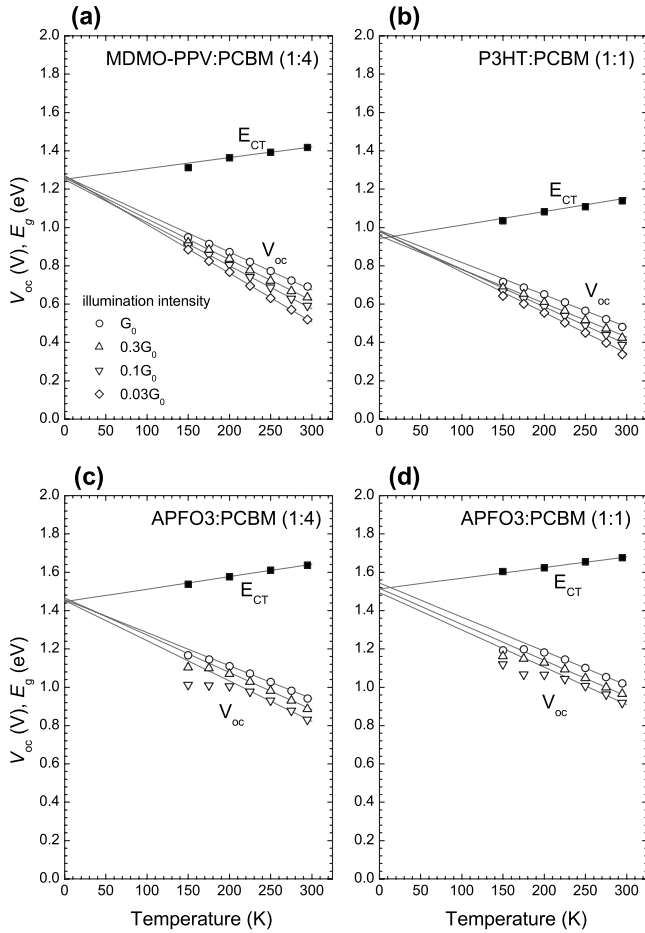


FIG. 4.  $V_{oc}$  and  $E_{CT}$  in function of temperature.  $E_{CT}$  is represented as the filled squares.  $V_{oc}$  was measured for different illumination intensities. The highest illumination intensity was  $G_0$ , about 0.1 sun, represented by open circles. The other illumination intensities are  $0.3G_0$  (open triangles up),  $0.1G_0$  (open triangles down) and  $0.03G_0$  (diamonds).  $E_{CT}$  and  $V_{oc}$  are linearly extrapolated to 0 K in their linear range, from  $\sim 200$  to 300 K. These curves are shown as black lines. Both these extrapolations result in the same value.

made for the relation between  $V_{oc}$  and the band gap of the used inorganic material.<sup>37</sup> This indicates that, with respect to  $V_{oc}$ , the energy of the CT exciton  $E_{CT}$  fulfills the same role as the band gap does in inorganic solar cells. This confirms that  $E_{CT}$  is an appropriate definition for the gap of organic solar cells based on blends of donor and acceptor materials. Note that  $E_{CT}$  is defined differently in this work than it is in previous work,<sup>18</sup> where we used an empirical definition for the interfacial band gap, i.e., the peak energy of the CT band minus two times the width of its Gaussian fit. The effective band gap defined in that work can be related to  $E_{CT}$ , as defined in this work as being  $4\sqrt{2kT\lambda} - \lambda$  lower. At room temperature and with  $\lambda$  ranging between 0.2–0.3 eV, this makes our previously defined effective band gap  $\sim 0.2$  eV lower than  $E_{CT}$ . However we believe that  $E_{CT}$ , as defined in the present work, represents the true energy of the CT state rather than the empirically defined effective band gap in Ref. 18 or the peak energy of CT emission.<sup>19,21</sup>

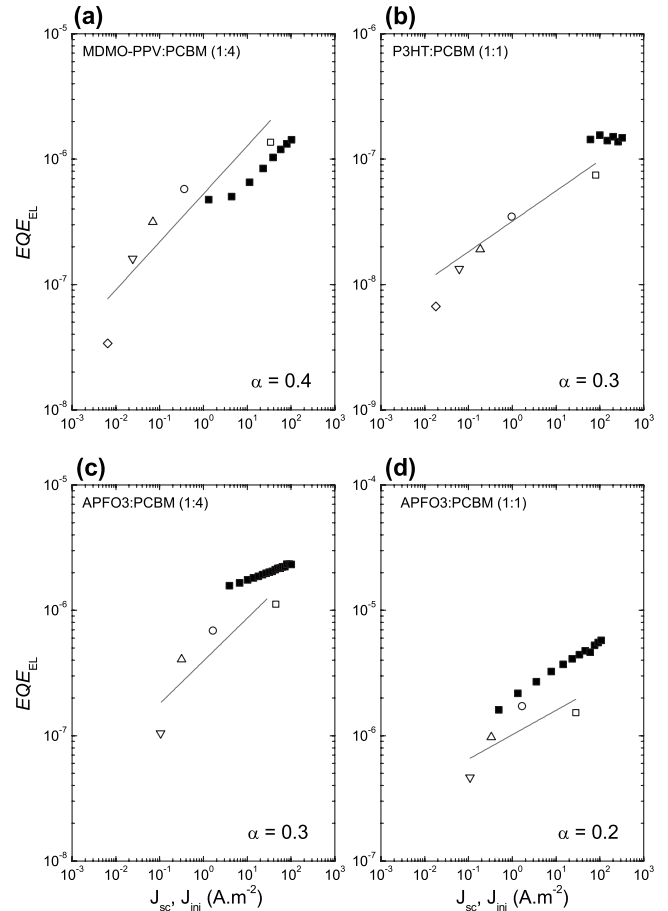


FIG. 5. The calculated and measured  $EQE_{EL}$ . The open symbols represent  $EQE_{EL}$  versus  $J_{sc}$ , calculated from  $V_{oc}$  measurements with the aid of formula (9). The filled squares are measurements of  $EQE_{EL}$  versus  $J_{inj}$ . The full lines represent a power-law dependence of  $EQE_{EL}$  on  $J_{sc}$  with a power  $\alpha$ .

## V. ILLUMINATION INTENSITY DEPENDENCE OF $V_{oc}$

We can calculate  $EQE_{EL}$  using expression (9), together with experimentally obtained values for  $V_{oc}$ ,  $J_{sc}$ ,  $E_{CT}$ , and  $f$ . In Fig. 5 the calculated values are shown as a function of the short-circuit current  $J_{sc}$  of the device. It can be seen that the calculated  $EQE_{EL}$  values are in the order of  $10^{-6}$  to  $10^{-9}$  with the lowest  $EQE_{EL}$  values for the P3HT:PCBM (1:1) devices.

In order to compare these calculated  $EQE_{EL}$  values with experimental values we have measured  $EQE_{EL}$  as a function of injection current, using a Si photodiode. Because of the low  $EQE_{EL}$  values, good signals have only been obtained at high injection currents. Because at  $V_{oc}$ , the photocurrent and injected current balance, the  $EQE_{EL}$  obtained by using formula (9) must be compared with experimentally measured  $EQE_{EL}$  at an injection current corresponding to the short-circuit current. In Fig. 5, it can be seen that the experimentally obtained  $EQE_{EL}(J_{inj})$  trend corresponds fairly well with the calculated  $EQE_{EL}(J_{sc})$ .

A dependence of  $EQE_{EL}$  on  $J_{inj}$  and thus internal charge density is observed. We can approximate the relation of  $EQE_{EL}$  as a function of  $J_{inj}$  by a power-law relationship

$$EQE_{EL}(J_{inj}) \approx EQE_{EL}(1)J_{inj}^{\alpha}. \quad (10)$$

Hereby is  $EQE_{EL}(1)$  the  $EQE_{EL}$  measured at an injection current of  $1 \text{ A}\cdot\text{m}^{-2}$ . This implies that  $J_0$ , as defined in Eq. (8), depends on the number of charges present in the device,

$$J_0(J_{inj}) \approx J_0(1)J_{inj}^{-\alpha}. \quad (11)$$

Hereby does  $J_0(1)$  equal  $J_0$  obtained by evaluating Eq. (8) for  $EQE_{EL}(1)$ . Inserting this expression in Eq. (5) gives for  $V \gg \frac{kT}{q}$ ,

$$J_{inj} = J_{0,n} \exp\left(\frac{qV}{nkT}\right). \quad (12)$$

Hereby  $n=1+\alpha$  and  $J_{0,n}=[J_0(1)]^{1/n}$ . For the material systems investigated in this work, we find values for  $n$  between 1 and 1.5.

Using Eq. (12), the expression for  $V_{oc} \gg \frac{kT}{q}$  becomes

$$V_{oc} = \frac{nkT}{q} \ln\left(\frac{J_{sc}}{J_{0,n}}\right). \quad (13)$$

In formula (13),  $J_{0,n}$  can be considered constant as opposed to  $J_0$  in Eq. (6). Relations of this type including an ideality factor  $n$  have been used before to describe the illumination intensity of  $V_{oc}$  of organic solar cells.<sup>9,26,32,33</sup> The factor  $n$  finds its origin in the fact that nonradiative recombination mechanisms are present and that these mechanisms depend differently on the charge density or injected current as compared to the radiative recombination mechanism. This causes  $EQE_{EL}$  to depend on the injected current. The exact nonradiative recombination mechanisms are not known at present but are currently under investigation. A third-order charge-carrier decay mechanism was found by at least three independent groups.<sup>38–41</sup> Further elucidation on these polaron recombination mechanisms is of high importance as their reduction will cause an increase in  $EQE_{EL}$  and  $V_{oc}$ .

## VI. VOLTAGE LOSSES IN POLYMER:FULLERENE SOLAR CELLS AT AM1.5 CONDITIONS

We will now do a more detailed study of the energetic losses  $q\Delta V$  between  $qV_{oc}$  and the gap  $E_{CT}$  under solar conditions. In analogy to Ref. 12, this loss can be seen as consisting of two parts,  $q\Delta V_{rad}$  and  $q\Delta V_{non-rad}$ . Equation (9) allows us to calculate these losses,

$$q\Delta V_{rad} = -kT \ln\left(\frac{J_{sc}h^3c^2}{fq2\pi(E_{CT}-\lambda)}\right), \quad (14)$$

$$q\Delta V_{nonrad} = -kT \ln(EQE_{EL}). \quad (15)$$

When all recombination is radiative CT emission,  $EQE_{EL}=1$  and  $\Delta V_{nonrad}$  vanishes. In this case  $\Delta V$  equals  $\Delta V_{rad}$ , a loss due solely to radiative emission. It is logarithmically dependent on properties of the CTC and incident light intensity ( $\sim J_{sc}$ ). For a given donor/acceptor pair with fixed  $E_{CT}$ ,  $\lambda$ , and  $f$ , this term is constant and represents a minimum loss between  $E_{CT}$  and  $qV_{oc}$  for a perfect device in which the only recombination mechanism present is a radiative one. Because of the logarithmical dependence the variation in parameters  $E_{CT}$  and  $\lambda$  will not affect this loss much.

TABLE II. Radiative and nonradiative energetic losses at  $V_{oc}$  for solar illumination and at room temperature. The radiative losses were calculated from the FTPS spectra. The nonradiative losses are related to  $EQE_{EL}$ .

	$\Delta V$ (V)	$\Delta V_{rad}$ (V)	$\Delta V_{nonrad}$ (V)
MDMO-PPV:PCBM (1:4)	0.58	0.24	0.34
P3HT:PCBM (1:1)	0.53	0.11	0.42
APFO3:PCBM (1:4)	0.59	0.24	0.35
APFO3:PCBM (1:1)	0.59	0.25	0.34

However the parameter  $f$  can be varied over several decades by varying the electronic coupling between polymer and fullerene. Choosing donor/acceptor pairs with a CT state which has a reduced coupling to the ground state will result in a decreased  $f$  and  $\Delta V_{rad}$ . The question remains if such a reduced coupling is achievable in future material systems without this having a disadvantageous influence on charge transfer and subsequent photocurrent generation.<sup>42</sup>

The part which takes into account the nonradiative recombination mechanisms, omnipresent in real devices, is reflected in the term  $\Delta V_{nonrad}$ . This term becomes larger than zero if  $EQE_{EL}$  is smaller than unity. As seen above, this part is also logarithmically dependent on  $J_{sc}$ , as  $EQE_{EL} \sim J_{sc}^\alpha$  for the polymer:fullerene solar cells we have investigated. Similar formulas were derived for the  $V_{oc}$  of inorganic solar cells but assumed to be valid for all solar cells operating in quasiequilibrium conditions.<sup>37</sup> It is argued that while  $\Delta V_{rad}$  is a thermodynamically unavoidable loss mechanism for a given material system,  $\Delta V_{nonrad}$  can in principle be avoided by reducing the nonradiative recombination paths. We experimentally find  $EQE_{EL}$  at room temperature in the range from  $10^{-9}$  to  $10^{-6}$ , when using Ca/Al and ITO/PEDOT:PSS contacts. Using non-Ohmic contacts will decrease the value of  $EQE_{EL}$  even further. For Si and GaAs solar cells,  $EQE_{EL}$  values are in the range of  $10^{-3}$ .<sup>37</sup> The question remains if these values can also be achieved for polymer:fullerene solar cells.

In Table II the loss factors are shown for the four investigated devices with ITO/PEDOT:PSS bottom contacts and Ca/Al top contacts under solar conditions. The overall offset  $\Delta V$  is fairly constant, with a value between 0.5 and 0.6 V. The P3HT:PCBM system has a lower value for  $f$  than the other (noncrystalline) polymer:PCBM systems. This results in a lower radiative loss  $\Delta V_{rad}$ . However in this system, there is no net benefit of this lower  $\Delta V_{rad}$  because  $\Delta V_{nonrad}$  is higher as compared to the other material systems. The reason for this higher  $\Delta V_{nonrad}$  and lower  $EQE_{EL}$  in P3HT:PCBM is not clear yet. However, a fairly constant total  $\Delta V$  is found for all four material systems. This explains the widely observed relation between  $V_{oc}$  and the difference between HOMO(D) and LUMO(A) for polymer:fullerene bulk heterojunction solar cells for this difference correlates with  $E_{CT}$ .<sup>23</sup>

## VII. CONCLUSION

In this work, CTC parameters are related to  $V_{oc}$ . It was shown that the free-energy difference  $E_{CT}$  between excited

CTC and ground state CTC is an appropriate definition of donor:acceptor blend gap. This parameter is independent of the measurement method. It can be measured as the symmetry point of CT absorption and emission or by fitting either the CT band in the absorption or  $EQE_{PV}$  spectrum or in the PL or EL spectrum. Its extrapolation to 0 K coincides with the extrapolation of  $V_{oc}$  to 0 K and the activation energy of the dark current. This is in analogy with the band gaps of several inorganic solar cells. For the material blends P3HT:PCBM, APFO3:PCBM and MDMO-PPV:PCBM  $E_{CT}$  is found to be slightly temperature dependent, with  $E_{CT}$  increasing with increasing temperature.

A formula for the open-circuit voltage  $V_{oc}$  in function of the CTC properties  $E_{CT}$ ,  $\lambda$ , and  $f$  as well as the temperature  $T$ , the short-circuit current  $J_{sc}$ , and the EL external quantum efficiency  $EQE_{EL}$  is deduced and shown to be valid for four polymer:fullerene bulk heterojunction solar cells. We show further that  $EQE_{EL}$  is not constant but depends on the injected current and thus on the number of charge carriers present in the device. This phenomenon is the origin of the ideality factor  $n$ , often used in the fitting of dark IV curves of organic solar cells.

The energetic losses between  $E_{CT}$  and  $qV_{oc}$  at room temperature and AM1.5 illumination conditions are around 0.5–0.6 eV for the investigated blends. The origin of these losses is twofold. About  $\sim 0.25$  eV of this loss is due to unavoidable radiative losses, related to properties of the CTC formed between polymer donor and fullerene acceptor.  $\sim 0.35$  eV is due to nonradiative losses. As these last terms represent a major loss factor for the devices investigated in this work, identification and possibly removal of the nonradiative decay paths are crucial in the future development of donor/acceptor based organic solar cells.

#### ACKNOWLEDGMENTS

We acknowledge the institute for the promotion of science and technology in Flanders (IWT-Vlaanderen), the Swedish Energy Agency for funding through the program Tandem, and Mats R. Andersson at Chalmers University for supplying us APFO3. Dirk Vanderzande and Wibren D. Oosterbaan are thanked for valuable discussions.

#### APPENDIX: DERIVATION OF EQ. (7)

In Eq. (7),

$$J_0 = \frac{q}{EQE_{EL}} \int EQE_{PV}(E) \phi_{BB}^T dE. \quad (A1)$$

We use expression (4) for  $EQE_{PV}$ ,

$$EQE_{PV}(E) = \frac{f}{E\sqrt{4\pi\lambda kT}} \exp\left(\frac{-(E_{CT} + \lambda - E)^2}{4\lambda kT}\right). \quad (A2)$$

If  $E \gg kT$ , the black body spectrum at temperature  $T$  can be approximated by

$$\phi_{BB}^T = \frac{2\pi}{h^3 c^2} E^2 \exp\left(-\frac{E}{kT}\right). \quad (A3)$$

We get for  $J_0$ ,

$$J_0 = \frac{q}{EQE_{EL}} \frac{2\pi}{h^3 c^2} f \int \frac{E}{\sqrt{4\pi\lambda kT}} \times \exp\left(\frac{-(E_{CT} - E + \lambda)^2}{4\lambda kT}\right) \exp\left(\frac{-E}{kT}\right) dE. \quad (A4)$$

Collecting both exponentials in one exponential function gives

$$J_0 = \frac{q}{EQE_{EL}} \frac{2\pi}{h^3 c^2} f \int \frac{E}{\sqrt{4\pi\lambda kT}} \times \exp\left(-\frac{(E_{CT} - E + \lambda)^2 + 4\lambda E}{4\lambda kT}\right) dE. \quad (A5)$$

We will concentrate on the term within the exponential. Working out the quadrate gives

$$J_0 = \frac{q}{EQE_{EL}} \frac{2\pi}{h^3 c^2} f \int \frac{E}{\sqrt{4\pi\lambda kT}} \times \exp\left(-\frac{(E_{CT} - E)^2 + 2\lambda(E_{CT} - E) + \lambda^2 + 4\lambda E}{4\lambda kT}\right) dE. \quad (A6)$$

Rearrangement of the terms gives

$$J_0 = \frac{q}{EQE_{EL}} \frac{2\pi}{h^3 c^2} f \int \frac{E}{\sqrt{4\pi\lambda kT}} \times \exp\left(-\frac{(E_{CT} - E)^2 - 2\lambda(E_{CT} - E) + \lambda^2 + 4\lambda E_{CT}}{4\lambda kT}\right) dE. \quad (A7)$$

This can also be written as

$$J_0 = \frac{q}{EQE_{EL}} \frac{2\pi}{h^3 c^2} f \exp\left(\frac{-E_{CT}}{kT}\right) \int \frac{E}{\sqrt{4\pi\lambda kT}} \times \exp\left(\frac{-(E_{CT} - E - \lambda)^2}{4\lambda kT}\right) dE. \quad (A8)$$

The expression under the integral sign is a normalized Gaussian peaking at  $E_{CT} - \lambda$ , multiplied by the photon energy  $E$ . Integrating this function will give a value close to the peak of the Gaussian, i.e.,  $E_{CT} - \lambda$ . This gives expression (8) for  $J_0$ ,

$$J_0 \approx \frac{q}{EQE_{EL}} f \frac{2\pi}{h^3 c^2} (E_{CT} - \lambda) \exp\left(-\frac{E_{CT}}{kT}\right). \quad (A9)$$

- \*Present address: Biomolecular and Organic Electronics, Center of Organic Electronics (COE), Department of Physics, Chemistry and Biology, Linköping University, 58183 Linköping, Sweden; koeva@ifm.liu.se
- <sup>1</sup>B. C. Thompson and J. M. J. Fréchet, *Angew. Chem., Int. Ed.* **47**, 58 (2008).
- <sup>2</sup>G. Dennler, M. C. Scharber, and C. J. Brabec, *Adv. Mater.* **21**, 1323 (2009).
- <sup>3</sup>S. H. Park, A. Roy, S. Beaupré, S. Cho, N. Coates, J. S. Moon, D. Moses, M. Leclerc, K. Lee, and A. J. Heeger, *Nature Photon.* **3**, 297 (2009).
- <sup>4</sup>H.-Y. Chen, J. H. Hou, S. Q. Zhang, Y. Y. Liang, G. W. Yang, Y. Yang, and G. Li, *Nature Photon.* **3**, 649 (2009).
- <sup>5</sup>Y. Y. Liang, Z. Xu, J. B. Xia, S.-T. Tsai, Y. Wu, G. Li, C. Ray, and L. Yu, *Adv. Mater.* (to be published).
- <sup>6</sup>M. C. Scharber, D. Muhlbacher, M. Koppe, P. Denk, C. Waldauf, A. J. Heeger, and C. J. Brabec, *Adv. Mater.* **18**, 789 (2006).
- <sup>7</sup>A. Gadisa, M. Svensson, M. R. Andersson, and O. Inganäs, *Appl. Phys. Lett.* **84**, 1609 (2004).
- <sup>8</sup>V. D. Mihailetschi, P. W. M. Blom, J. C. Hummelen, and M. T. Rispens, *J. Appl. Phys.* **94**, 6849 (2003).
- <sup>9</sup>B. P. Rand, D. P. Burk, and S. R. Forrest, *Phys. Rev. B* **75**, 115327 (2007).
- <sup>10</sup>K. Vandewal, K. Tvingstedt, A. Gadisa, O. Inganäs, and J. V. Manca, *Nat. Mater.* **8**, 904 (2009).
- <sup>11</sup>W. Shockley and H. Queisser, *J. Appl. Phys.* **32**, 510 (1961).
- <sup>12</sup>U. Rau, *Phys. Rev. B* **76**, 085303 (2007).
- <sup>13</sup>L. Goris, A. Poruba, L. Hod'áková, M. Vanecek, K. Haenen, M. Nesladek, P. Wagner, D. Vanderzande, L. D. Schepper, and J. V. Manca, *Appl. Phys. Lett.* **88**, 052113 (2006).
- <sup>14</sup>J. J. Benson-Smith, L. Goris, K. Vandewal, K. Haenen, J. V. Manca, D. Vanderzande, D. D. C. Bradley, and J. Nelson, *Adv. Funct. Mater.* **17**, 451 (2007).
- <sup>15</sup>M. A. Loi, S. Toffanin, M. Muccini, M. Forster, U. Scherf, and M. Scharber, *Adv. Funct. Mater.* **17**, 2111 (2007).
- <sup>16</sup>M. Hallermann, S. Haneder, and E. D. Como, *Appl. Phys. Lett.* **93**, 053307 (2008).
- <sup>17</sup>T. Drori, C. X. Sheng, A. Ndobe, S. Singh, J. Holt, and Z. V. Vardeny, *Phys. Rev. Lett.* **101**, 037401 (2008).
- <sup>18</sup>K. Vandewal, A. Gadisa, W. D. Oosterbaan, S. Bertho, F. Banishoeib, I. V. Severen, L. Lutsen, T. J. Cleij, D. Vanderzande, and J. V. Manca, *Adv. Funct. Mater.* **18**, 2064 (2008).
- <sup>19</sup>D. Veldman, O. Ipek, S. C. J. Meskers, J. Sweelssen, M. M. Koetse, S. C. Veenstra, J. M. Kroon, S. S. van Bavel, J. Loos, and R. A. J. Janssen, *J. Am. Chem. Soc.* **130**, 7721 (2008).
- <sup>20</sup>Y. Zhou, K. Tvingstedt, F. Zhang, C. Du, W.-X. Ni, M. R. Andersson, and O. Inganäs, *Adv. Funct. Mater.* **19**, 3293 (2009).
- <sup>21</sup>K. Tvingstedt, K. Vandewal, A. Gadisa, F. Zhang, J. V. Manca, and O. Inganäs, *J. Am. Chem. Soc.* **131**, 11819 (2009).
- <sup>22</sup>D. Veldman, S. C. J. Meskers, and R. A. J. Janssen, *Adv. Funct. Mater.* **19**, 1939 (2009).
- <sup>23</sup>P. Panda, D. Veldman, J. Sweelssen, J. J. A. M. Bastiaansen, B. M. W. Langeveld-Voss, and S. C. J. Meskers, *J. Phys. Chem. B* **111**, 5076 (2007).
- <sup>24</sup>M. D. Perez, C. Borek, S. R. Forrest, and M. E. Thompson, *J. Am. Chem. Soc.* **131**, 9281 (2009).
- <sup>25</sup>W. J. Potscavage, A. Sharma, and B. Kippelen, *Acc. Chem. Res.* **42**, 1758 (2009).
- <sup>26</sup>V. Dyakonov, *Appl. Phys. A: Mater. Sci. Process.* **79**, 21 (2004).
- <sup>27</sup>R. A. Marcus, *J. Phys. Chem.* **93**, 3078 (1989).
- <sup>28</sup>I. R. Gould, D. Noukakis, L. Gomez-Jahn, R. H. Young, J. L. Goodman, and S. Farid, *Chem. Phys.* **176**, 439 (1993).
- <sup>29</sup>N. S. Sariciftci, *Primary Photoexcitations in Conjugated Polymers: Molecular Exciton Versus Semiconductor Band Model* (World Scientific Publishing Company, Singapore, 1997).
- <sup>30</sup>L. Goris, K. Haenen, M. Nesladek, P. Wagner, D. Vanderzande, L. D. Schepper, J. D'Haen, L. Lutsen, and J. V. Manca, *J. Mater. Sci.* **40**, 1413 (2005).
- <sup>31</sup>C. G. Shuttle, A. Maurano, R. Hamilton, B. O'Regan, J. C. de Mello, and J. R. Durrant, *Appl. Phys. Lett.* **93**, 183501 (2008).
- <sup>32</sup>C. Waldauf, M. C. Scharber, P. Schilinsky, J. A. Hauch, and C. J. Brabec, *J. Appl. Phys.* **99**, 104503 (2006).
- <sup>33</sup>W. J. Potscavage, S. Yoo, and B. Kippelen, *Appl. Phys. Lett.* **93**, 193308 (2008).
- <sup>34</sup>K. Kanemoto, I. Akai, H. Hashimoto, T. Karasawa, N. Negishi, and Y. Aso, *Phys. Status Solidi C* **6**, 193 (2009).
- <sup>35</sup>G. Wantz, L. Hirsch, N. Huby, L. Vignau, A. S. Barrière, and J. P. Parneix, *J. Appl. Phys.* **97**, 034505 (2005).
- <sup>36</sup>M. O. Osotov, V. V. Bruevich, and D. Y. Paraschuk, *J. Chem. Phys.* **131**, 094906 (2009).
- <sup>37</sup>M. A. Green, *Prog. Photovoltaics* **11**, 333 (2003).
- <sup>38</sup>C. Deibel, A. Baumann, and V. Dyakonov, *Appl. Phys. Lett.* **93**, 163303 (2008).
- <sup>39</sup>C. Shuttle, B. O'Regan, A. Ballantyne, J. Nelson, D. Bradley, J. D. Mello, and J. Durrant, *Appl. Phys. Lett.* **92**, 093311 (2008).
- <sup>40</sup>C. G. Shuttle, B. O'Regan, A. M. Ballantyne, J. Nelson, D. D. C. Bradley, and J. R. Durrant, *Phys. Rev. B* **78**, 113201 (2008).
- <sup>41</sup>G. Juška, K. Genevičius, N. Nekrašas, G. Sliužys, and G. Dennler, *Appl. Phys. Lett.* **93**, 143303 (2008).
- <sup>42</sup>J. L. Bredas, J. E. Norton, J. Cornil, and V. Coropceanu, *Acc. Chem. Res.* **42**, 1691 (2009).